The large mean body size of mammalian herbivores explains the productivity paradox during the last glacial maximum

Dan Zhu[1*], Philippe Ciais[1], Jinfeng Chang[1,2], Gerhard Krinner[3], Shushi Peng[4], Nicolas Viovy[1], Josep Peñuelas[5], Sergey Zimov[6]

[1] Laboratoire des Sciences du Climat et de l'Environnement, LSCE CEA CNRS UVSQ, 91191 Gif Sur Yvette, France
[2] Sorbonne Universités (UPMC), CNRS-IRD-MNHN, LOCEAN/IPSL, 4 place Jussieu, 75005 Paris, France
[3] CNRS, Univ. Grenoble Alpes, Institut de Géosciences de l'Environnement (IGE), Grenoble, France
[4] Sino-French Institute for Earth System Science, College of Urban and Environmental Sciences, Peking University, Beijing 100871, China
[5] CSIC, Global Ecology Unit, CREAF-CSIC, Universitat Autònoma de Barcelona, Bellaterra, 08193 Catalonia, Spain
[6] Northeast Science Station, Pacific Institute for Geography, Russian Academy of Sciences, Cherskii 678830, Russia

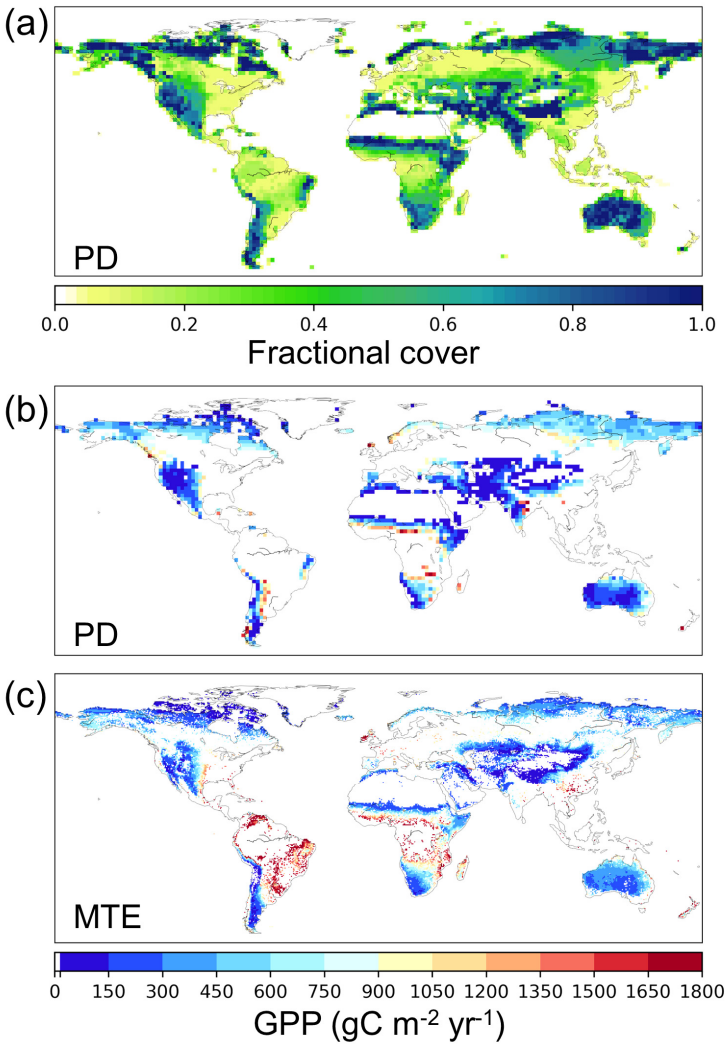

Supplementary Figure 1. Modelled present-day grassland fractional cover and GPP. (a) Simulated fractional cover of grass for PD (1960-2009 mean). (b) Simulated mean annual GPP during 1960-2009 for grass-dominated grid cells (simulated grass coverage larger than 50% at 2° resolution). (c) Mean annual GPP during 1999-2008 from the data-driven MTE GPP[1] with a spatial resolution of 0.5º, shown only for the pixels classified as grasses and shrubs in the SYNMAP land cover product[2].

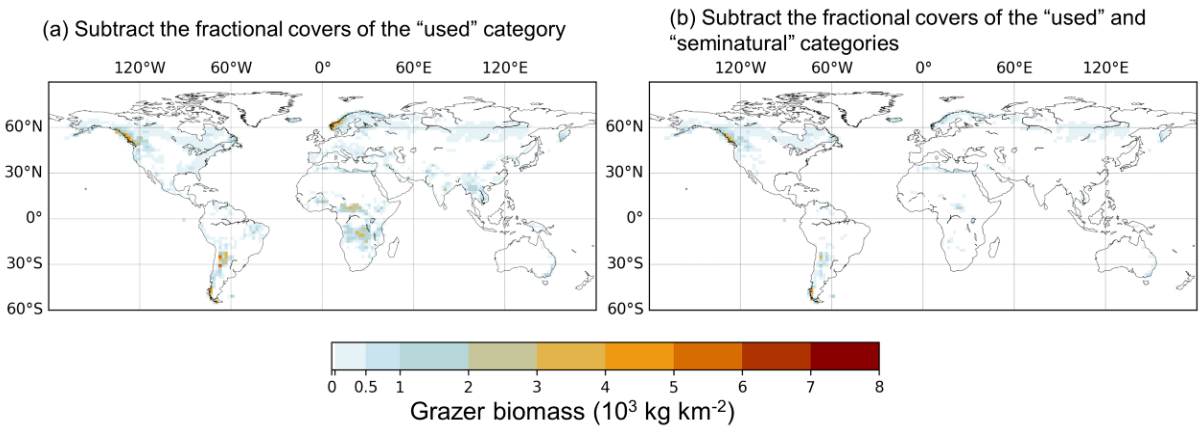

Supplementary Figure 2. Modelled large grazer biomass density for present-day, excluding human land use, according to the Anthromes version 2 map[3] which separated three major categories: Used, Seminatural, and Wild. The fractional covers of the Used category **(a)** or Used + Seminatural categories **(b)** are subtracted from the simulated potential grazer density as shown in Fig. 2a.

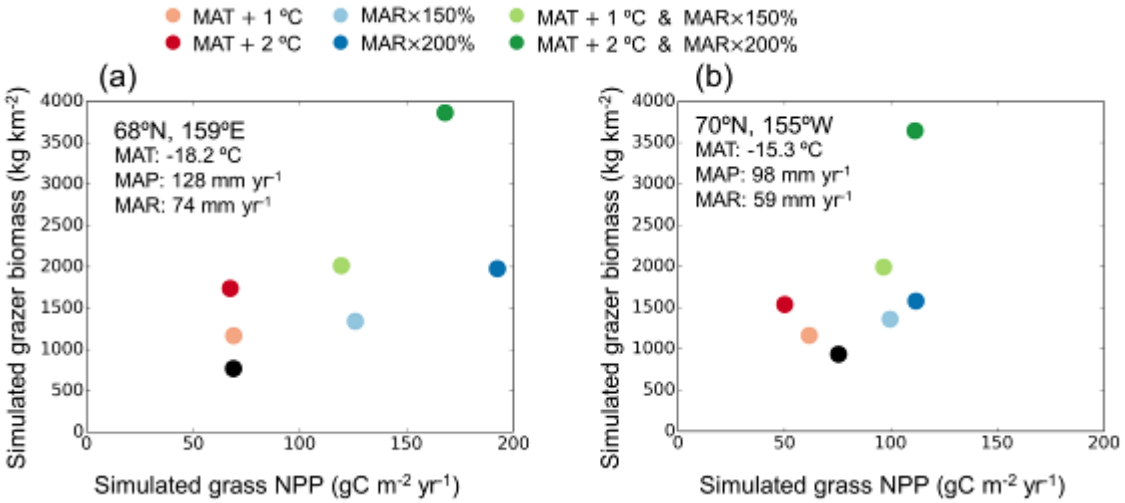

Supplementary Figure 3. Sensitivity of grazer biomass density to temperature and rainfall for the two grid cells corresponding to the study areas in Zimov et al.[4] (a) and Mann et al.[5] (b). The black dots indicate the results forced by the original climate forcing (labelled in each subplot: MAT: mean annual temperature; MAP: mean annual precipitation including rainfall and snowfall; MAR: mean annual rainfall). The colored dots indicate the results if the climate forcing is modified: red: temperature at each time step increase by 1 or 2 °C; blue: rainfall at each time step (only when temperature>0 °C) multiplied by 1.5 or 2; green: combined increase in temperature and rainfall.

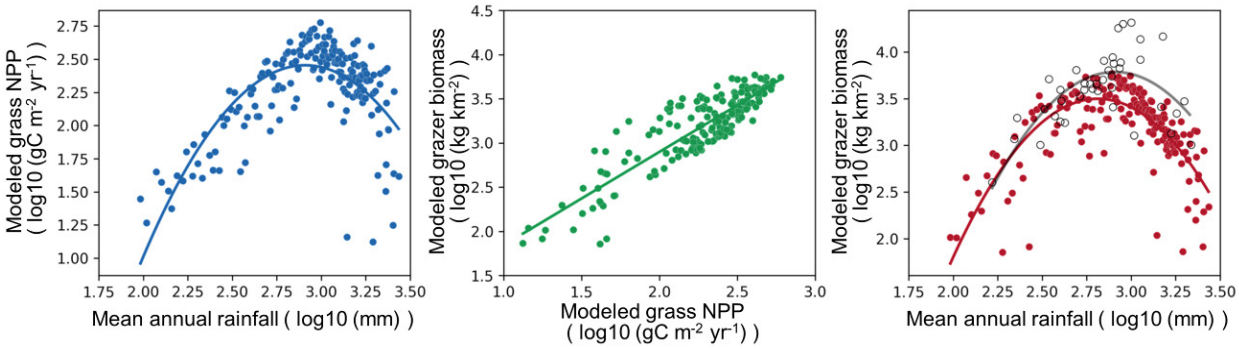

Supplementary Figure 4. The same figure as Fig. 4a but separated in 2-D.

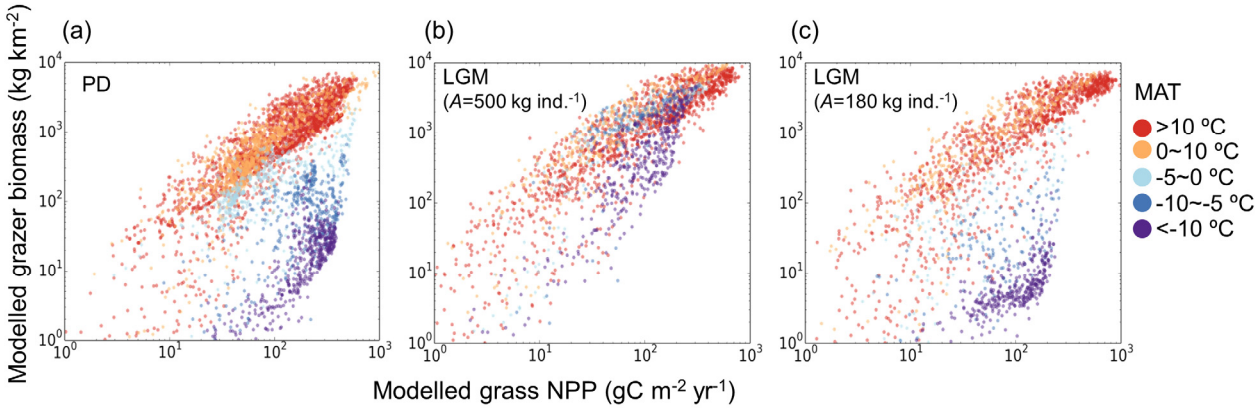

Supplementary Figure 5. Relationship between grass NPP and grazer biomass under different mean annual temperatures (MATs). Points represent modelled results across all grid cells on land for present-day (PD, a), and for the LGM (b and c) prescribed with different grazer body size (*A*) for the two runs, 500 and 180 kg ind.$^{-1}$, the former derived from the reconstructions by Mann et al.[5] and Zimov et al.[4] based on the relative bone abundance of different taxa, the latter the same as that for PD in the northern hemisphere according to Hatton et al.[6].

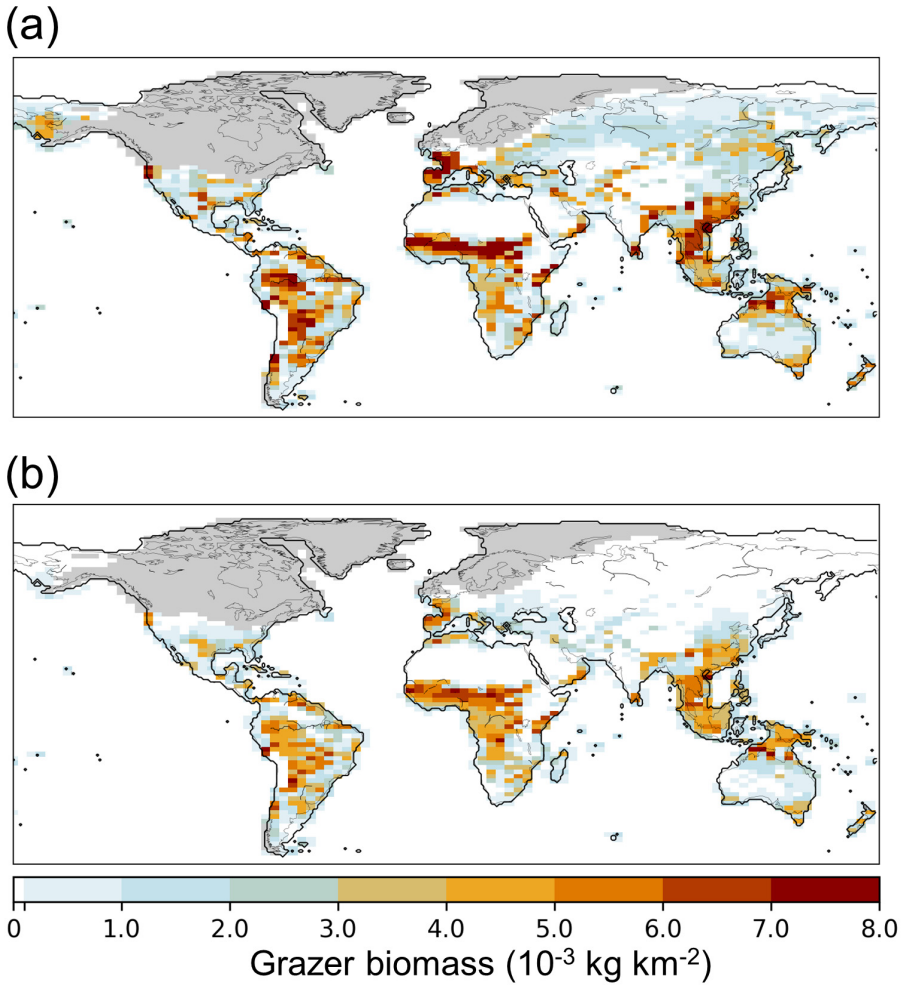

Supplementary Figure 6. Simulated grazer biomass density for the LGM with different prescribed body sizes. (a) The same as Fig. 3c except for the globe, namely, body size is prescribed as 500 kg ind.$^{-1}$, according to reconstructions by Mann et al.[5] and Zimov et al.[4] (b) Body size is set to 180 kg ind.$^{-1}$ as a sensitivity test, the same as present-day. Grey areas indicate ice sheet during the LGM using the map from the PMIP3 protocol.

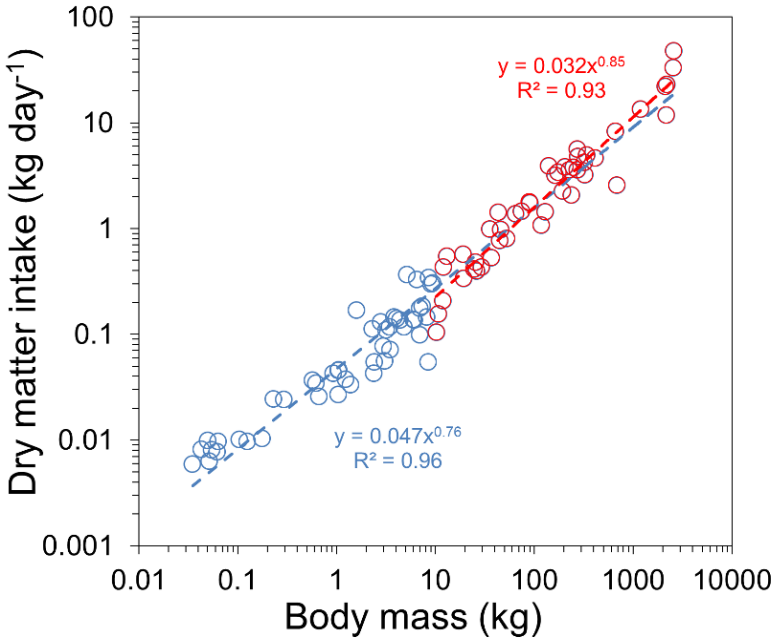

Supplementary Figure 7. Correlation of body mass and dry matter intake rate for mammalian herbivores. The data were compiled in Clauss et al.[7] Blue circles indicate all the 93 herbivorous mammals compiled in ref[7], while red circles indicate the subset of 46 large herbivores with body mass larger than 10 kg. The allometric regression equation of the subset of large herbivores gives a higher exponent (0.85).

Supplementary Table 1. Herbivore biomass density of protected areas in Africa and Asia, and ecosystems in North America, calculated from the raw data provided by Hatton et al.[6] The data for another 15 ecosystems in North America[8] (Messier, 1994) cited in Hatton et al.[6] were not used in this study, since they only included one herbivore species (moose).

Name of Ecosystem	Area (km^2)	Latitude	Longitude	Herbivore biomass ($kg\ km^{-2}$)
Africa				
Amboseli National Park, Kenya	390	-2.68	37.30	14192
Etosha National Park, Namibia	45140	-19.02	15.78	250
Gonarezhou National Park, Zimbabwe	5053	-21.91	32.00	5647
Hluhluwe iMfolozi National Park, South Africa	960	-28.28	31.92	7592
Hwange National Park, Zimbabwe	14596	-19.08	26.56	2778
Kalahari National Park, South Africa	9590	-25.73	20.39	258
Katavi National Park, Tanzania	4471	-6.88	31.22	7763
Kidepo Valley National Park, Uganda	1442	3.88	33.78	2191
Kruger National Park, South Africa	18989	-23.99	31.58	3002
Lake Manyara National Park, Tanzania	97	-3.58	35.81	18736
Masai Mara National Reserve, Kenya	1585	-1.51	35.09	6539
Mkomazi Game Reserve, Tanzania	3245	-4.19	38.28	1868
Nairobi National Park, Kenya	120	-2.05	32.58	3743
Ngorongoro Crater, Tanzania	260	-3.17	35.57	14070
Nwaswitshaka River, Kruger NP, South Africa	81	-24.91	31.84	3913
Okavango Delta, Botswana	1	-19.30	22.96	6934
Pilanesburg National Park, South Africa	500	-25.27	27.04	3188
Queen Elizabeth National Park, Uganda	1978	-0.22	29.97	11823
Sabie River, Kruger NP, South Africa	17	-25.05	31.72	9075
Savuti area of Chobe National Park, Botswana	300	-18.60	24.58	4354
Selous Game Reserve, Tanzania	43626	-8.81	37.44	5070
Serengeti ecosystem, Tanzania	25000	-2.39	34.88	2875
Tarangire National Park, Tanzania	2072	-4.15	36.11	3297
Asia				
Bandhavgarh National Park, India	449	23.62	80.41	2084
Bandipur National Park, India	890	11.76	76.45	9775
Bhadra Wildlife Sanctuary, India	492	13.48	75.62	1930
Bori-Satpura Tiger Reserve, India	1428	22.51	78.27	1218
Buxa Tiger Reserve, India	369	26.63	89.54	2168
Corbett Tiger Reserve, India	1319	29.53	78.94	4009
Kalakad Mundanthurai Tiger Reserve, India	895	8.51	77.47	1538
Kanha National Park, India	940	22.29	80.56	3332
Phen Wildlife Sanctuary, India	110	22.29	80.56	953
Melghat Tiger Reserve, India	1677	21.45	77.17	1502
Nagarahole National Park, India	643	12.04	76.14	9994
Nagarjunasagar-Srisailam Sanctuary, India	3568	16.09	78.72	366
Palamau Tiger Reserve, India	1014	23.86	84.35	2998
Panna National Park, India	542	24.32	80.54	923
Pench Tiger Reserve (MR), India	257	21.57	79.47	1857
Pench Tiger Reserve (MP), India	758	21.62	79.47	1449
Periyar Tiger Reserve, India	777	9.49	77.21	4980
Ranthambhore National Park, India	393	26.01	76.49	2919
Sariska Tiger Reserve, India	866	27.32	76.44	2291
Similipal Tiger Reserve, India	845	21.80	86.34	5249
Sunderbans Tiger Reserve, India	1600	21.94	88.90	1502

Tadoba-andhari Tiger Reserve, India	625	20.24	79.40	1549
Bardia National Park, Nepal	968	28.31	81.43	4549
Sikhote-Alin Zapovednik, Russia	3985	48.00	138.00	390
Taman Negara National Park (Kuala Koh), Malaysia	200	4.70	102.47	5822
North America				
Denali Park, Alaska		63.61	-150	70
East-central Ontario		47.15	-82	359
Interior Alaska		63.31	-150	69
Isle Royale, Michigan		48.04	-89	507
Jasper Park, Alberta		52.94	-118	174
North-central Canada		60.25	-101	495
North-central Minnesota		47.89	-94	429
Northeast Alberta		55.79	-111	69
Northeast Minnesota		47.22	-92	389
Northern Alberta		57.38	-111	64
South-central Ontario		48.81	-84	90
Southern Quebec		45.79	-75	300
Southwest Manitoba		51.76	-101	504
Southwest Quebec		46.85	-76	90
West-central Yukon		63.47	-138	54

Supplementary Table 2. Present-day (PD) and pre-industrial (PI) global and regional total grazer biomass (unit: million tonnes live weight) simulated by ORCHIDEE-MICT. The model simulates natural vegetation without anthropogenic land use, and thus potential values. The gridded fractional covers of the categories "Wild" and "Seminatural" from Antromes version 2[3] for the year 2000 and 1900 were multiplied to the PD and PI potential values, in order to estimate the reduction of wild large grazers due to human land use, with the relative reductions listed in parenthesis.

		Africa	Asia	South America	North America	Europe	Australia	Globe
PD (1960-2009 mean)	Potential	47	22	18	17	14	9.8	128
	Remnants on Wild lands	1.1 (98%)	1.4 (94%)	1.9 (89%)	3.5 (79%)	0.6 (96%)	0.2 (98%)	8.7 (93%)
	Remnants on Wild and Seminatural lands	8.6 (82%)	4.8 (78%)	4.7 (74%)	5.5 (68%)	3 (79%)	0.5 (95%)	27 (79%)
PI (1860-1899 mean)	Potential	56	22	23	16	12	8.8	138
	Remnants on Wild lands	3.2 (94%)	1.5 (93%)	8.4 (63%)	5.2 (68%)	0.7 (94%)	4.1 (53%)	23 (83%)
	Remnants on Wild and Seminatural lands	28 (50%)	12 (45%)	20 (13%)	11 (31%)	4.8 (60%)	6.1 (31%)	82 (41%)

Supplementary Note 1. Subtraction of tropical rainforest from simulated potential large grazer density

The current model, lacking an explicit representation of browsers and mixed feeders, produced a significant distribution of potential large grazers in densely forested areas, in particular in the tropical rainforests (Supplementary Fig. 8a). This is because the grazing module is primarily driven by grass productivity, and the grasses in tropical forested areas, although with a very small simulated fractional land cover (ca. 10%), are highly-productive under the favourable climatic conditions and can still support some grazers (ca. 1000 kg km^{-2}, Supplementary Fig. 8b) in the model. In reality, large herbivores in tropical rainforests are mainly generalist feeders like elephants, feeding on both grass and browse plants[9]; whereas conventional grazers do not usually live in the rainforest (with a few exceptions like capybaras in South America). To alleviate this model drawback, we subtracted the fractional covers of tropical rainforest, according to the empirically-derived potential natural vegetation map[10], from the direct model output of potential grazer density (Supplementary Fig. 8a), and thus derived Fig. 2a and the total regional/global values listed in Supplementary Table 1. We did not do similar subtractions for boreal and temperate forests, because: 1) these forests are not totally closed due to disturbances from extreme weather events like drought, frost and storms, fires, pathogen outbreaks[11,12], and potentially, large herbivores. The fractional tree cover in these forests seldom exceeds 80%, according to the remote sensing-derived product of vegetation continuous field[13]; and 2) some large grazer species can indeed live in the northern forests, such as aurochs[14], the extinction of which has been attributed to human hunting and expulsion[15]. Still, our model may have overestimated grazer density in non-tropical dense forests, because most large herbivore species inhabiting forests are mixed feeders and browsers, which are missing in the current model.

For the LGM results, no such subtraction was applied either, considering the very limited distribution of dense forests (e.g. areas with modelled tree cover > 0.8 accounted for only 6% of total land area for the tropics, in contrast to 42% in the present-day simulation).

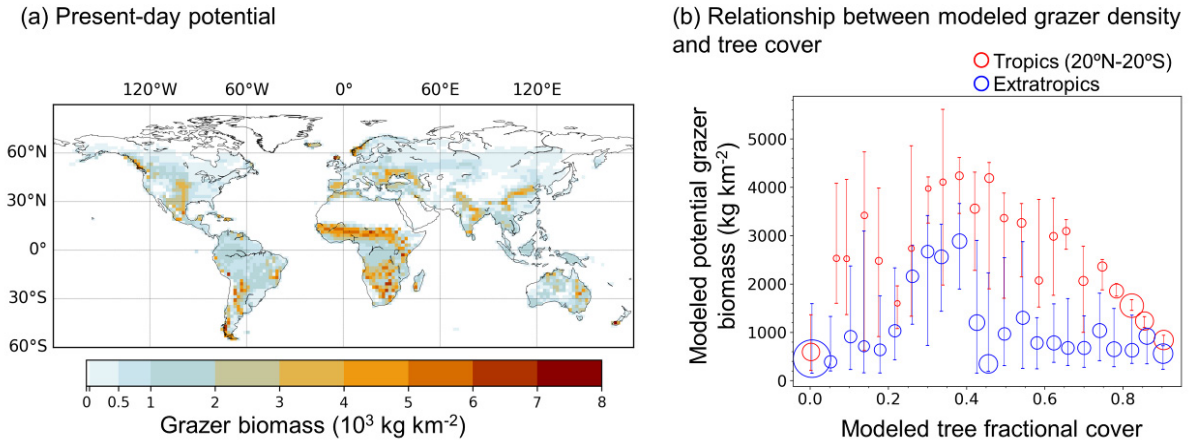

Supplementary Figure 8. (a) Modelled potential large grazer biomass density for present-day (1960-2009 mean), without post-processing. **(b)** Relationship between modelled grazer biomass density and tree cover for present-day. Grid cells in tropical and extratropical regions were divided into tree cover bins of 0.04, with the circles representing median values and the error bars indicating 25^{th} - 75^{th} percentiles for each bin. The size of each circle is proportionate to the number of pixels in each bin.

Supplementary Note 2. Conversion from the modelled plant functional types (PFTs) into mega-biomes

In order to facilitate comparison between modelled LGM vegetation distribution and reconstructions based on pollen and plant macrofossil data from BIOME 6000 version 4.2 (available online: http://www.bridge.bris.ac.uk/resources/Databases/BIOMES_data), we used a method similar to that of Prentice et al.[16] and Kageyama et al.[17] to convert modelled vegetation properties into the 9 "mega-biomes" provided by BIOME 6000. The algorithm is shown in Supplementary Fig. 9: firstly, the global vegetation is divided between cold biomes and the rest, with the threshold GDD5 (annual growing degree days above 5 ºC) equalling to 350 K days; secondly, the separation between forest/savanna, dry grassland/shrubland, and desert (or between forest/dry tundra and tundra) depends on the modelled total foliage projective cover (*FPC*), which is a function of both fractional cover and leaf area index (*LAI*) of each PFT ($FPC = V \times (1 - e^{-0.5 \times LAI})$); thirdly, forest and savanna (or forest and dry tundra) are separated by the average height of all existing tree PFTs; finally, within the forest, the dominance of particular tree PFTs is used to separate tropical, temperate and boreal forests. After the conversion, only one biome is assigned to each grid cell. This conversion algorithm makes use of not only modelled PFT fractional covers, but also *FPC* and average height, which relates to modelled *LAI* and woody biomass and ultimately relates to vegetation productivity and allocation in the model. Thus it enables the distinction between the relatively more productive dry tundra (corresponding to graminoid and forb tundra, see Table 3 in Harrison and Prentice[18]) and the low productive tundra (corresponding to cushion forb tundra, erect dwarf shrub tundra, etc.) in Siberia and Alaska.

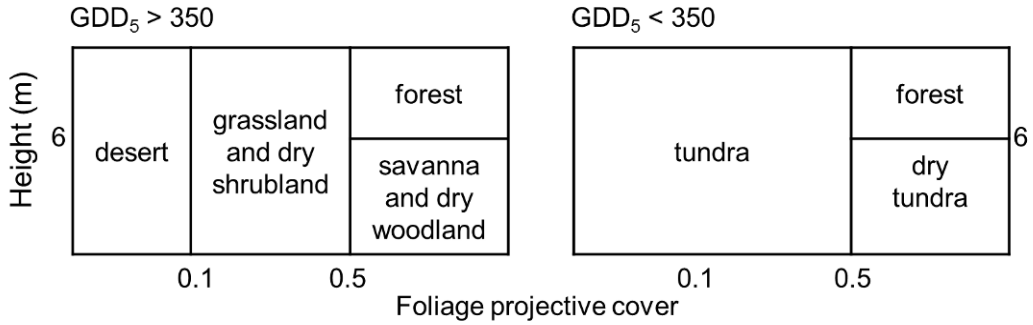

	Forest
Tropical tree PFTs dominant?	tropical forest
Temperate broadleaf evergreen PFT dominant?	warm temperate forest
Temperate tree PFTs dominant?	temperate forest
The rest	boreal forest

Supplementary Figure 9. Algorithm to convert the modelled PFT properties into the 9 mega-biomes provided by BIOME 6000, adapted from Prentice et al.[16] and Kageyama et al.[17]

Supplementary discussion. Impacts of grazing on land carbon cycle during the LGM.

As shown in Fig. 5, total aboveground grass consumption by grazers was 1.7 Pg C yr^{-1}, or 3.2% of the total body weight in the unit of dry matter intake per day, which is within the empirical range for domestic livestock (2-4%)[19]. Modelled global mean ratio of grazer-to-grass biomass was 0.5% (in g C m^{-2} : g C m^{-2}), comparable to the estimate of 0.8% for the ratio of terrestrial herbivore-to-primary producer biomass by Harfoot et al.[20] using the Madingley ecosystem model, knowing that their result included all plant-eating animals, not only the large mammalian grazers considered in this study. Our result is also within the range of an empirical estimate of 1.1±0.7% for the herbivore-to-primary producer biomass ratio in temperate and tropical grasslands[21].

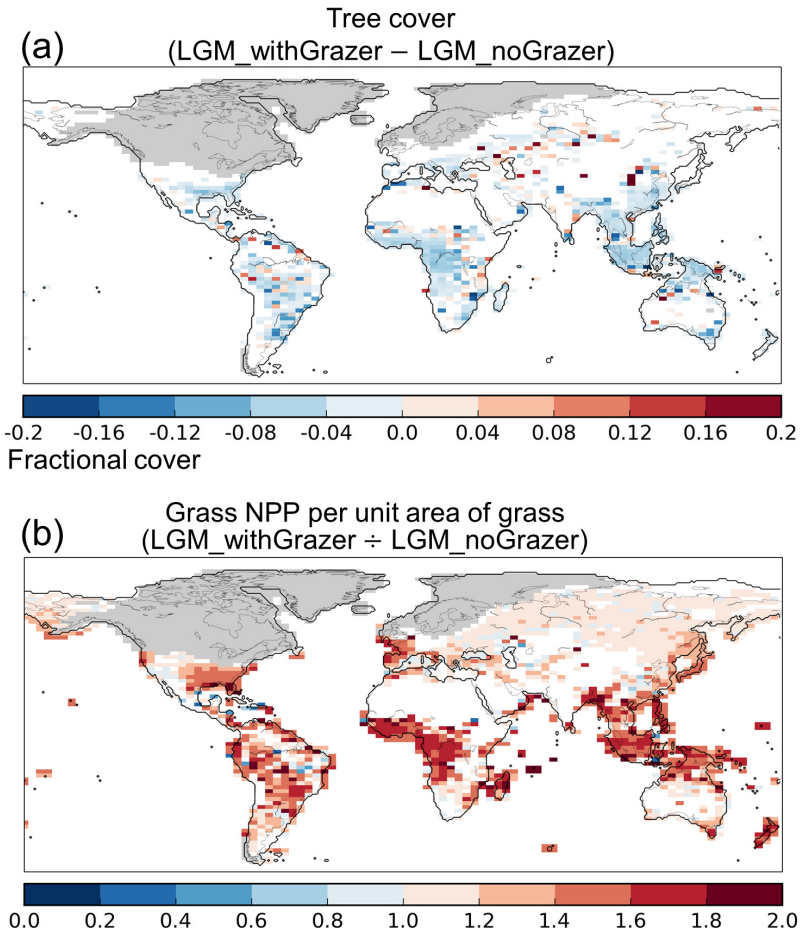

Supplementary Figure 10. Impacts of grazing on tree cover and grassland productivity at the LGM. **(a)** Difference of tree fractional cover between LGM-withGrazer and LGM-noGrazer.

(b) Ratio of grass NPP (gC m^{-2}grassland yr^{-1}) between LGM-withGrazer and LGM-noGrazer. In order to separate the effect of changing grass fractional cover, we plotted grass NPP per unit area of grass instead of per unit area of ground ("grass NPP" elsewhere in this study refers to the latter).

Supplementary Fig. 10 displays the difference in tree cover and grassland productivity between model results with and without grazers. The difference in tree cover showed a general reduction with grazing (Supplementary Fig. 10a), mainly due to the trampling-induced tree mortality (equation (10) in Methods). In the model, grazers also have an indirect positive impact on the trees through the interaction between fire and vegetation, because grazing reduces grass fuel load and thus the frequency of fires[22,23], which leads to smaller fire-induced tree mortalities. The slight increase of tree fractional cover in few grid cells (Supplementary Fig. 10a) corresponded to the areas where grazers favour trees by causing a reduction of fire occurrence that exceeds the negative effects of trampling in the model.

The suppression of woody plants by large grazers and the subsequent alteration in landscape structure has been observed in modern exclosure experiments and paleoecological records[24]. A remote-sensing observation in Kruger National Park in South Africa shows an average change of woody cover (vegetation > 1 m tall) from 20% to 12%, or 40% reduction, in areas accessible to herbivores, compared to the areas of long-term herbivore exclusions[25]. Among the herbivores with different body size, elephants have been revealed as the primary agent of treefall in savannas, due to their physical strength and height causing disproportionate mortality of shrubs and maturing trees[24,26]; while smaller herbivores, especially browsers, increase mortalities of tree saplings and suppress tree regeneration[27]. Our model results show a general reduction of 5-10% absolute tree fractional cover in tropical and sub-tropical regions with the simulated grazer density during the LGM (Supplementary Fig. 10a), close to the observed reduction in ref[25]. In contrast, simulations with the LPJ-GUESS model over Africa with a parameterization of wild grazers[23] showed no significant changes in vegetation distribution with and without grazers. This is partly because of the different parameterizations of trampling effect, as we calibrated the trampling-induced tree mortality (equation (10)) to match the mortality caused by elephants[28], while in LPJ-GUESS, which did not yet include a herbivore functional type to represent elephants, the trampled area by grazers was used to calculate the decrease of tree saplings[23], which may underestimate the disproportionate effect of elephants compared to the one of smaller wild herbivores[26].

Grazing increased grass NPP per unit area of grass in most of the grid cells (Supplementary Fig. 10b), with larger increments in areas of higher grazer biomass density, indicating that the positive effects of grazers on grass NPP in the model, i.e. the regrowth of more productive young leaves after defoliation and the higher photosynthesis capacities (a process simply calibrated from herbivore exclusion experiments to approximate the positive effects associated with accelerated nutrient cycling and traits/composition changes - see Methods), outweighed the negative effect of biomass removal by grazing. The above- to belowground ratio of global grass NPP increased from 1.2 in the LGM without grazers to 1.3 with grazers,

due to more allocation of assimilated carbon to leaves to compensate for defoliation in our model[29]. Such a preferential allocation to the shoot system compared to roots in response to defoliation is supported by experimental evidence[30]. As for grass standing biomass, total aboveground biomass was slightly smaller with grazers (5.2 Pg C) than without grazers (5.4 Pg C), resulting from intake being not fully compensated by a higher NPP; while belowground biomass increased from 4.2 Pg C without grazers to 6.6 Pg C with grazers due to a higher NPP.

References

1. Jung, M. *et al.* Global patterns of land-atmosphere fluxes of carbon dioxide, latent heat, and sensible heat derived from eddy covariance, satellite, and meteorological observations. *J. Geophys. Res.* **116,** G00J07 (2011).

2. Jung, M., Henkel, K., Herold, M. & Churkina, G. Exploiting synergies of global land cover products for carbon cycle modeling. *Remote Sens. Environ.* **101,** 534–553 (2006).

3. Ellis, E. C., Klein Goldewijk, K., Siebert, S., Lightman, D. & Ramankutty, N. Anthropogenic transformation of the biomes, 1700 to 2000. *Glob. Ecol. Biogeogr.* **19,** no-no (2010).

4. Zimov, S. A., Zimov, N. S., Tikhonov, A. N. & Iii, F. S. C. Mammoth steppe : a high-productivity phenomenon. *Quat. Sci. Rev.* **57,** 26–45 (2012).

5. Mann, D. H., Groves, P., Kunz, M. L., Reanier, R. E. & Gaglioti, B. V. Ice-age megafauna in Arctic Alaska: extinction, invasion, survival. *Quat. Sci. Rev.* **70,** 91–108 (2013).

6. Hatton, I. A. *et al.* The predator-prey power law: Biomass scaling across terrestrial and aquatic biomes. *Science (80-.).* **349,** aac6284-aac6284 (2015).

7. Clauss, M., Schwarm, A., Ortmann, S., Streich, W. J. & Hummel, J. A case of non-scaling in mammalian physiology? Body size, digestive capacity, food intake, and ingesta passage in mammalian herbivores. *Comp. Biochem. Physiol. Part A Mol. Integr. Physiol.* **148,** 249–265 (2007).

8. Messier, F. Ungulate Population Models with Predation: A Case Study with the North American Moose. *Ecology* **75,** 478 (1994).

9. Hempson, G. P., Archibald, S. & Bond, W. J. A continent-wide assessment of the form and intensity of large mammal herbivory in Africa. *Science (80-.).* **350,** 1056–1061 (2015).

10. Ramankutty, N. & Foley, J. A. Estimating historical changes in global land cover: Croplands from 1700 to 1992. *Global Biogeochem. Cycles* **13,** 997–1027 (1999).

11. Reichstein, M. *et al.* Climate extremes and the carbon cycle. *Nature* **500,** 287–295 (2013).

12. Thurner, M. *et al.* Evaluation of climate-related carbon turnover processes in global vegetation models for boreal and temperate forests. *Glob. Chang. Biol.* **23,** 3076–3091 (2017).

13. Defries, R.S., M.C. Hansen, F.G. Hall, G.J. Collatz, B.W. Meeson, S.O. Los, E.Brown De Colstoun, and D.R. Landis. 2009. ISLSCP II Continuous Fields of Vegetation Cover, 1992-1993. ORNL DAAC, Oak Ridge, Tennessee, USA. https://doi.org/10.3334/ORNLDAAC/931.

14. Bocherens, H., Hofman-Kamińska, E., Drucker, D. G., Schmölcke, U. & Kowalczyk, R. European Bison as a Refugee Species? Evidence from Isotopic Data on Early Holocene Bison and Other Large Herbivores in Northern Europe. *PLoS One* **10,** e0115090 (2015).

15. Van Vuure, C. Retracing the Aurochs: History, Morphology and Ecology of an extinct wild Ox. Pensoft Publishers. Sofia-Moscow. ISBN 954-642-235-5 (2005).

16. Prentice, I. C., Harrison, S. P. & Bartlein, P. J. Global vegetation and terrestrial carbon cycle changes after the last ice age. *New Phytol.* **189,** 988–98 (2011).

17. Kageyama, M. *et al.* Mid-Holocene and last glacial maximum climate simulations with the IPSL model: part II: model-data comparisons. *Clim. Dyn.* **40,** 2469–2495 (2013).

18. Harrison, S. P. & Prentice, C. I. Climate and CO2 controls on global vegetation distribution at the last glacial maximum: analysis based on palaeovegetation data, biome modelling and palaeoclimate simulations. *Glob. Chang. Biol.* **9,** 983–1004 (2003).

19. IPCC (2006) 2006 IPCC Guidelines for National Greenhouse Gas Inventories, Prepared by the National Greenhouse Gas Inventories Programme (eds Eggleston HS,

Buendia L, Miwa K, Ngara T, Tanabe K). IGES, Japan.

20. Harfoot, M. B. J. *et al.* Emergent Global Patterns of Ecosystem Structure and Function from a Mechanistic General Ecosystem Model. *PLoS Biol.* **12,** e1001841 (2014).

21. Cebrian, J. *et al.* Producer nutritional quality controls ecosystem trophic structure. *PLoS One* **4,** 1–5 (2009).

22. Sinclair, A. R. E. *et al.* Long-Term Ecosystem Dynamics in the Serengeti: Lessons for Conservation. *Conserv. Biol.* **21,** 580–590 (2007).

23. Pachzelt, A., Forrest, M., Rammig, A., Higgins, S. I. & Hickler, T. Potential impact of large ungulate grazers on African vegetation, carbon storage and fire regimes. *Glob. Ecol. Biogeogr.* **24,** 991–1002 (2015).

24. Bakker, E. S. *et al.* Combining paleo-data and modern exclosure experiments to assess the impact of megafauna extinctions on woody vegetation. *Proc. Natl. Acad. Sci.* **113,** 847–855 (2016).

25. Asner, G. P. *et al.* Large-scale impacts of herbivores on the structural diversity of African savannas. *Proc. Natl. Acad. Sci.* **106,** 4947–4952 (2009).

26. Asner, G. P. & Levick, S. R. Landscape-scale effects of herbivores on treefall in African savannas. *Ecol. Lett.* **15,** 1211–1217 (2012).

27. Staver, A. C. & Bond, W. J. Is there a 'browse trap'? Dynamics of herbivore impacts on trees and grasses in an African savanna. *J. Ecol.* **102,** 595–602 (2014).

28. Dublin, H. T., Sinclair, A. R. E. & McGlade, J. Elephants and Fire as Causes of Multiple Stable States in the Serengeti-Mara Woodlands. *J. Anim. Ecol.* **59,** 1147 (1990).

29. Krinner, G. *et al.* A dynamic global vegetation model for studies of the coupled atmosphere-biosphere system. *Global Biogeochem. Cycles* **19,** (2005).

30. Caldwell, M. M., Richards, J. H., Johnson, D. A., Nowak, R. S. & Dzurec, R. S. Coping with herbivory: Photosynthetic capacity and resource allocation in two semiarid Agropyron bunchgrasses. *Oecologia* **50,** 14–24 (1981).